ACS OMEGA

http://pubs.acs.org/journal/acsodf
Article

Controllable Drug-Release Ratio and Rate of Doxorubicin-Loaded Natural Composite Films Based on Polysaccharides: Evaluation of Transdermal Permeability Potential

Ji Ha Lee,* Hiroya Tsubota, and Tomoyuki Tachibana

Cite This: *ACS Omega* 2024, 9, 1936−1944

ABSTRACT: In drug delivery systems, it is crucial to develop a drug carrier capable of regulating both the drug-release rate and the drug-release ratio. This study proposes a method for controlling the drug-release ratio/rate using doxorubicin-loaded natural composite films composed of polysaccharides (cellulose, chitin, chitosan, or cellulose nanocrystal) and mineral substances (MMT: montmorillonite). We succeeded in controlling the doxorubicin release ratio from 25 to 88% depending on the natural polysaccharide. Likewise, the reduction rate differed depending on the type of natural polysaccharide, whereas the reduction in release was achieved by mixing MMT. Cellulose had the largest reduction in the drug release ratio, approximately 30%, and cellulose nanocrystals showed little change. Furthermore, we conducted a skin permeation test on the natural polysaccharide film with the highest release rate to confirm its transdermal permeability potential. The polysaccharide doxorubicin-loaded film sustainably released doxorubicin for 2 days, which indicated the potential of a carrier for DDS applications.

INTRODUCTION

Natural polysaccharide materials are mostly raw materials extracted from plants or seaweed that minimize chemical treatment or synthetic processes and have several advantages as sustainable materials.[1−3] In addition, because they have excellent biocompatibility and can contain various functionalities, safe and effective results can be expected in the field of drug delivery.[4−6] Furthermore, natural polysaccharides are nanofibers made up of a series of monosaccharides and offer processability and controllability as they can be processed into various forms, such as films, gels, and nanoparticles, while allowing for the modulation of drug-release rates and other physical properties to achieve desired outcomes.[7−9] Cellulose is the most abundant natural polysaccharide and is a primary component of plant cell walls. It exhibits a strong structural characteristic and is composed of cellulose units arranged in a fibrous manner.[10−12] Chitosan, which is derived from the exoskeleton of crustaceans, is a polysaccharide polymer chain composed of partially acetylated glucosamine units. It possesses flexibility, strong bonding capabilities, and high biocompatibility.[13−16] Chitin is extracted from the peels, seeds, and other plant parts of fruits and vegetables.[17−19] Cellulose nanocrystal is characterized by its carboxyl-functionalized hydroxyl groups, an extremely fine fiber diameter of 3−4 nm width, and a high aspect ratio of more than 100.[20,21] It is derived from wood fibers, and it shows high purity while preserving a fibrous structure.[20−22] Cellulose nanocrystals contain numerous carboxyl groups with high chemical reactivity and can acquire negative charges under basic conditions. These negative charges interact with positively charged compounds, including metal ions and ionic liquids, facilitating the formation of novel self-assemblies.[23] Cellulose is a vital plant-derived carbohydrate with versatile industrial uses, while cellulose nanocrystals, derived from cellulose, possess unique traits and serve in advanced materials and biomedicine.[20−23]

Although they are based on saccharides, these polysaccharides having different types and positions of functional groups of saccharides are self-assembled under specific conditions and show differences in their properties when forming gels. For example, under water conditions, polysaccharides of the same concentration may be transparent (e.g., cellulose nanocrystal) or opaque such as cellulose, chitin, and chitosan. In addition, when the rheology of these polysaccharides is measured, there is a difference value in G' and G'', and even if they have similar G' and G'' values, they show different aspects depending on the change in strain %.[24−26] In this study, we gelatinize these natural polysaccharides and the anticancer drug doxorubicin to fabricate drug-loaded films. These natural polysaccharides are gelatinized by encapsulating doxorubicin, an anticancer drug, and prepared as a drug encapsulation film to control each drug-release ratio and drug-release rate. Using a hydrogel form as a drug carrier is appealing because it can encapsulate a desired amount of drug during gel formation. Gelator molecules self-assemble with each other through several noncovalent interactions such as hydrogen bonding, $\pi-\pi$ stacking, and electrostatic interaction to form a dense fibril network structure.[27,28] Doxorubicin stands out as one of the most effective chemotherapeutic drugs for cancer treatment.

Received: November 7, 2023
Revised: December 11, 2023
Accepted: December 14, 2023
Published: December 29, 2023

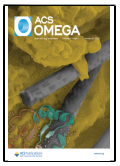

https://doi.org/10.1021/acsomega.3c08834
ACS Omega 2024, 9, 1936−1944

However, when used invasively, it not only targets cancer cells but also inflicts severe damage on normal healthy cells.[29] To tackle this issue, researchers have explored the potential of an injectable hydrogel,[30] which allows for the immobilization and targeted delivery of a substantial amount of drug molecules directly to the affected tissue.

Previous research on hydrogel drug carriers with doxorubicin highlights the control of drug release through factors like pH and temperature.[28−31] Self-assembled hydrogels, while effective, face challenges with continuous release. In contrast, releasing the drug in a film state maintains the form and enables controlled release by adjusting compound ratios, temperature, and reaction time.[32] The incorporation of montmorillonite (MMT), a mineral with remarkable adsorption capabilities, into natural polysaccharide-based drug delivery systems is explored.[33−42] MMT's ability to provide continuous drug release at a controlled concentration makes it promising for enhancing drug delivery. Studies on starch/MMT and chitosan/MMT composite films have demonstrated controlled release patterns influenced by the MMT content. Tailored drug-release strategies are crucial for addressing specific medical needs. Chronic conditions may require controlled and continuous release, while acute scenarios demand rapid drug release. This study introduces a drug-loaded natural composite hydrogel based on polysaccharides, incorporating a 2D sheet MMT to explore its impact on gelation, mechanical strength, and drug-release dynamics. The transdermal permeability potential of the resulting drug encapsulation film is also evaluated.

MATERIALS AND METHODS

Materials. In this study, five kinds of polysaccharides such as cellulose, chitin, chitosan, and cellulose nanocrystal were used. Each polysaccharide, cellulose, chitin, and chitosan we purchased was composed of nanofibers. A cellulose solution (2 wt % in water), a chitin solution (2 wt % in water), and a chitosan solution (2 wt % in water) were obtained from Sugino Machine Limited (Japan). A cellulose nanocrystal (2 wt % in water) was purchased from DKS Co. Ltd. (Japan). Dimethyl sulfoxide (DMSO, >99.0 wt %) and PBS (0.1 M, pH = 7), prepared using sodium dihydrogen phosphate (NaH_2PO_4) and disodium hydrogen phosphate (Na_2HPO_4) were purchased from FUJIFILM Wako Pure Chemical Corporation (Japan). Doxorubicin hydrochloride (>95.0%) as a model cancer cell treatment drug was purchased from Tokyo Chemical Industry Co., Ltd. (Japan). MMT was purchased from Sigma-Aldrich (USA). All the chemicals were used without further purification. The skin of a 7 week-old male hairless mouse, from which subcutaneous fat was removed, was purchased from Japan SLC, Inc. (Japan).

Preparation of Doxorubicin-Loaded Polysaccharide Hydrogels and Films with/without MMT. A cellulose solution, chitin nanofiber solution, and chitosan solution (2 wt %) of 500 mg were mixed each with water for a final volume of 50 μL to prepare a polysaccharide hydrogel. A cellulose nanocrystal solution (2 wt %) of 500 mg was mixed with water for a final volume of 500 μL to prepare a polysaccharide hydrogel. Doxorubicin was dissolved in DMSO to obtain a doxorubicin solution with an 8 mg/mL concentration. A 20 μL doxorubicin solution of 20 μL was added to the polysaccharide hydrogel to prepare doxorubicin-loaded polysaccharide hydrogels. For the preparation of doxorubicin-loaded polysaccharide hydrogels with MMT, MMT was dissolved in water to obtain an MMT solution with a concentration of 5 mg/mL, and the MMT solution of 50 μL was mixed with 20 μL of the doxorubicin solution to obtain the MMT/doxorubicin solution. The MMT/doxorubicin solution was stirred at 25 °C for 1 h to load the doxorubicin into the MMT. Subsequently, an MMT/doxorubicin solution of 70 μL was added to each polysaccharide hydrogel to prepare doxorubicin-loaded polysaccharide hydrogels with MMT. In the case of the polysaccharide hydrogel with/without MMT using cellulose nanocrystal, water was added to make a total volume of 500 μL. Other conditions were adjusted to achieve a total water volume of 50 μL. These doxorubicin-loaded polysaccharide hydrogels with/without MMT were kneaded with a spatula in an ointment container. The doxorubicin-loaded polysaccharide hydrogels with/without MMT were then kept at 25 °C for 24 h to obtain the corresponding doxorubicin-loaded polysaccharide films with/without MMT.[16] Each sample information on doxorubicin-loaded polysaccharide hydrogels with/without MMT is shown in Table S1.

Rheological Properties of the Hydrogels. The hydrogels containing doxorubicin were positioned onto a rheometer plate following the established protocol. Rheological evaluations were carried out using a dynamic shear rheometer (MCR102; Anton Paar GmbH, Graz, Austria) operating in dynamic oscillation mode employing a stainless-steel cone plate. A 1.0 mm spacing was maintained between the hydrogel and the plate, which had a diameter of 50 mm. Measurements were executed at a temperature of 25 °C. Frequency sweep examinations were conducted across the range of 1−100 Hz. Strain-sweep assessments were performed by progressively increasing the oscillation amplitude from 1 to 200% of the apparent shear strain at 1 Hz.

Drug−Release Testing of Doxorubicin-Loaded Polysaccharide Films. The doxorubicin-loaded polysaccharide films and the doxorubicin-loaded polysaccharide films containing MMT were assessed for drug release ratio utilizing an ultraviolet−visible spectrophotometer (UV−vis, V-750, JASCO Corp.) operating across the 200−700 nm spectrum. A quartz cell with a path length of 10 mm was employed for measurements. To fully immerse each film, 1.5 mL of PBS was introduced into the ointment container at room temperature. At specific intervals, 1.5 mL of PBS containing the released doxorubicin was extracted from the ointment container for subsequent analysis, and after measurement, it was returned to the container. The drug-release ratio was determined through eq 1, where R_L represents the doxorubicin loading amount within each film, and R_t signifies the quantity of doxorubicin released in 1.5 mL of PBS during each sampling period. The latter was quantified via a calibration curve established for free doxorubicin, measured at a wavelength of 478.5 nm (Figure S1).

$$\% \text{ Drug Release} = \frac{R_t}{R_L} \times 100 \quad (1)$$

All the release tests were carried out twice, and based on the experimental results, the drug release amount for the time change was divided into sections. Then, the slope values were organized to derive the experimental results.

Observation of the Doxorubicin-Loaded Polysaccharide Film. The doxorubicin-loaded polysaccharide hydrogels were produced using the identical procedure described above and were dispensed onto a microscope slide. Following this,

https://doi.org/10.1021/acsomega.3c08834
ACS Omega 2024, 9, 1936−1944

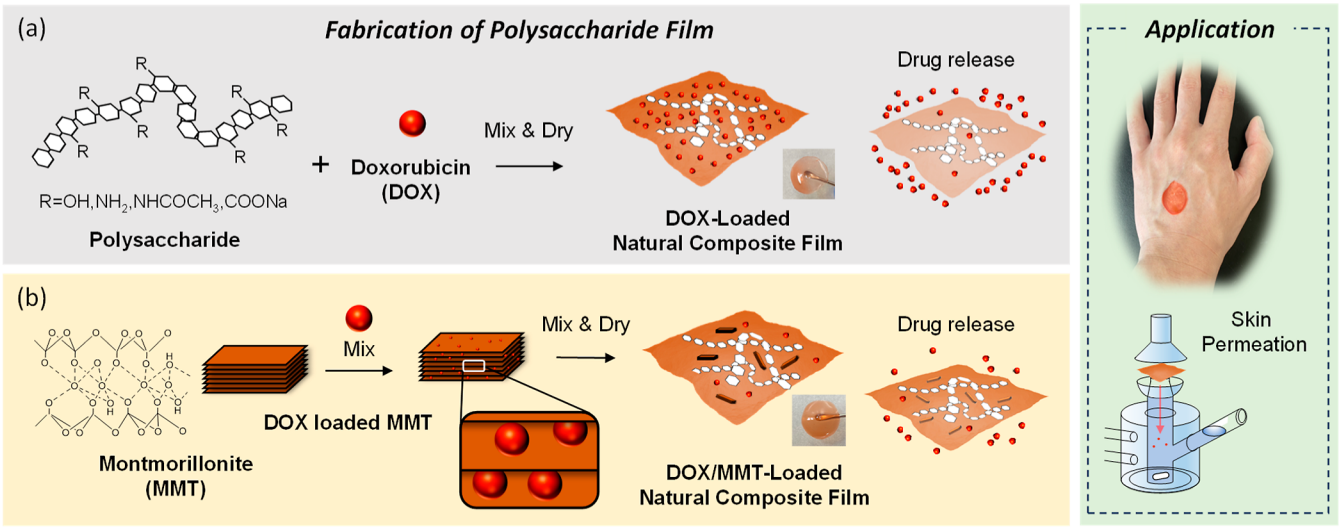

Figure 1. Illustration of the doxorubicin-loaded polysaccharide film (a) without and (b) with MMT and their application.

they were allowed to air-dry for a duration of 24 h at room temperature. This process yielded the doxorubicin-loaded polysaccharide film attached to the microscope slide. Scanning electron micrographs of the specimens were captured by using a field emission scanning electron microscope (Philips XL30 S FEG). The microscope was operated with an accelerating voltage ranging from 5 to 15 kV and an emission current of 10 μA. The samples for the top-view observation were examined without any additional manipulation.

Kinetic Models for the Analysis of the Drug-Release Mechanism. Kinetic models were used to analyze the drug-release mechanism from DOX-loaded polysaccharide films.[43−45] Zero-order (eq 2), first-order (eq 3), and Higuchi (eq 4) and Korsmeyer−Peppas models in eq 5 have been used.[46,47] In eqs 2−5, M_t denotes the quantity of drug released at distinct time points t, M_0 corresponds to the initial amount of drug present within the release medium (in this case, M_0 = 0), R_0 signifies the initial ratio of drug in the release medium (in this case, R_0 = 0), K_0 and K_1 are the zero- and first-order release constants, respectively, K_H is the Higuchi dissolution constant, K_{KP} stands for the Korsmeyer−Peppas rate constant, M_t/M_∞ signifies the percentage of drug released at specific time points t, and n is the diffusion exponent. The values of n serve to characterize the drug-release mechanism.

$$M_t = M_0 + K_0 t \tag{2}$$

$$\log\left(100 - \frac{M_t}{M_\infty} \times 100\right) = \log\left(100 - \frac{M_0}{M_\infty} \times 100\right) - K_1 t \tag{3}$$

$$M = K_H t^{0.5} \tag{4}$$

$$\frac{M_t}{M_\infty} = K_{KP} t^n \tag{5}$$

Values of "n" falling within the range of 0.5−1.0 signify non-Fickian diffusion, implying anomalous transport kinetics. Values around 0.5 indicate a process controlled by diffusion (Fickian diffusion), while values below 0.5 can arise from partial drug diffusion through the swollen matrix and water-filled pores present in the formulations.[34] The value of R^2 is the coefficient of determination in eq 6

$$R^2 = 1 - \frac{\sum_{i=1}^{m} (y_i - \hat{y}_i)^2}{\sum_{i=1}^{m} (y_i - \overline{y}_i)^2} \tag{6}$$

where y_i is the measured drug release ratio at specific time, $\hat{y}_i$ is the predicted drug release ratio calculated by each model in eqs 2−4, and $\overline{y}_i$ is the average of the measured drug release ratio. The value of R^2 close to 1 indicates a strong correlation between the model's predictions and the measured data. Conversely, the value of R^2 close to 0 indicates that the model does not adequately have correlation with measured data.

Evaluating the Penetration of Drug into the Skin. The evaluation of drug penetration into the skin was conducted using Franz diffusion cells (PermeGear, Inc.) equipped with a 5.0 mm diameter. A receptor chamber containing a 20 mM PBS solution at pH 7.4 was placed, and its temperature was maintained at 37 °C with continuous stirring at 600 rpm. Hairless mouse skin was positioned on the receptor chamber, and a film sample, previously soaked in water for 2 min, was applied onto the skin. Subsequently, a 10% aqueous solution of DMSO was added to the surface of the sample.[16] At 18, 24, and 48 h intervals, 200 μL of the solvent was collected from the receptor chamber and quantified using a fluorescence spectrometer (LS-55, PerkinElmer) to ascertain the amount of doxorubicin that had permeated the skin. Free doxorubicin was excited at 470 nm, and emission was measured at 550 nm to establish a calibration curve for determining the quantity of doxorubicin that had penetrated the skin. The experiment was conducted three times, and the best-fit curve was calculated employing the least-squares technique. Furthermore, the doxorubicin amount that had penetrated the skin was calculated using eqs 7 and 8 presented in the following formula: where A_{DS} (μg/cm^2) denotes the quantity of doxorubicin that had penetrated the skin per unit area of hairless mouse skin, A_m (μg) represents the doxorubicin amount that had permeated the skin, A_S (cm^2) signifies the area of hairless mouse skin, R_D (%) stands for the ratio of doxorubicin that penetrated the skin, and A_L (μg) denotes the loaded amount of doxorubicin in the film.

$$A_{DS} = \frac{A_m}{A_s} \tag{7}$$

https://doi.org/10.1021/acsomega.3c08834
ACS Omega 2024, 9, 1936−1944

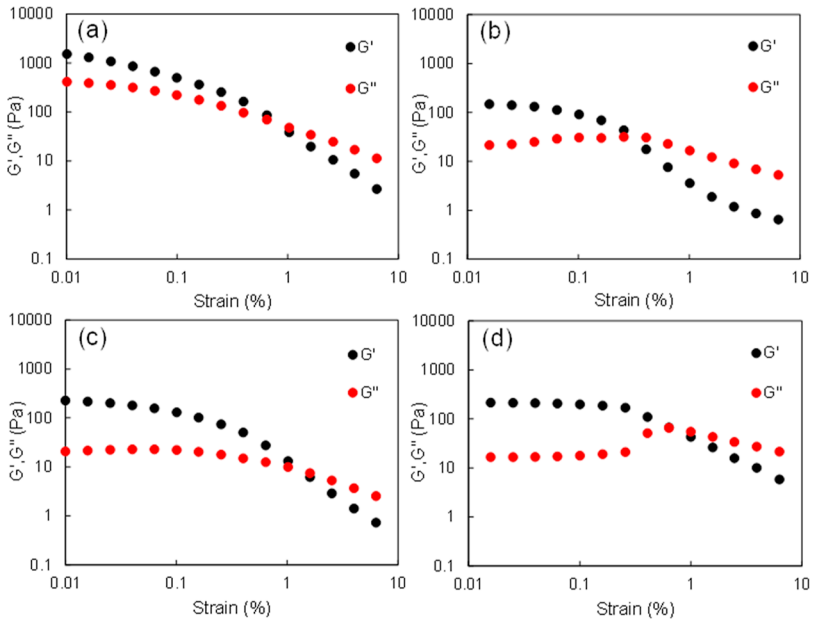

Figure 2. Strain sweeps at 0.01−10.00% (frequency = 0.6283 rads^{-1}) of doxorubicin-loaded polysaccharide hydrogels (n = 1): (a) cellulose, (b) chitin, (c) chitosan, and (d) cellulose nanocrystal.

$$R_D = \frac{A_m}{A_L} \times 100 \quad (8)$$

RESULTS AND DISCUSSION

Drug-Loaded Natural Composite Hydrogels Based on Polysaccharides and Their Rheological Properties. Doxorubicin-loaded polysaccharide hydrogels were prepared by adding doxorubicin to cellulose, chitin, chitosan, or ellulose nanocrystals (Figure 1). Except for the doxorubicin-loaded cellulose nanocrystal hydrogel, the doxorubicin-loaded polysaccharide hydrogels were opaque. The transparency of cellulose nanocrystals in water is due to their robust interaction with water molecules and the uniform dispersion which consists of fine particles.[20−22] Doxorubicin-loaded polysaccharide hydrogels with MMT were also prepared by adding doxorubicin to cellulose, chitin, chitosan, or cellulose nanocrystals (Figures 2 and S2).

To confirm the mechanical properties of doxorubicin-loaded polysaccharide hydrogels, the storage (G') and loss (G'') moduli were determined via rheometric measurement (Figure 2) and the values of these results, G'/G'' and reversed strain %, were calculated (Table 1). When G' and G'' are reversed in strain measurements during rheological measurements, the mechanical behavior of the material changes. Typically, when G' is greater than G'', the material is elastic and tends to retain its shape when subjected to external stress. On the other hand, if G'' is greater than G', the material is predominantly viscous and easier to change shape in response to external stress. The strain amplitude sweeps of the doxorubicin-loaded polysaccharide hydrogels demonstrated a different tendency depending on the polysaccharide. As a result of analyzing each of the G' and G'' moduli, the values of G'/G'' increased in the order of cellulose (G'/G'' = 5.05), chitin (G'/G'' = 7.94), chitosan (G'/G'' = 12.76), and cellulose nanocrystal (G'/G'' = 15.40). A large value of G'/G'' means that the gap between the G' moduli and the G'' moduli is large and that the gel is close to a solid behavior. Furthermore, the value of strain % was analyzed when G'/G'' < 1 is reversed. It was confirmed that the values of reversed strain % in chitin, cellulose nanocrystal, cellulose, and chitosan were increased. The strain % of the reverse point were 0.41, 1.00, 1.03, and 1.61 for chitin, cellulose nanocrystal, cellulose, and chitosan, respectively. In addition to contributing to drug adsorption and transport because of the 2D sheet structure of MMT, the rheometric measurement was carried out to confirm the effect on the mechanical strength of the doxorubicin-loaded polysaccharide hydrogel between nanofibers (Figure S3)—no significant difference in G'/G'' values of doxorubicin-loaded polysaccharide hydrogels with MMT compared to those without MMT. However, the doxorubicin-loaded cellulose hydrogels with MMT showed a lower strain % value when the G'/G'' value reversed less than 1, which may be related to the release rate. No significant changes were observed upon adding MMT. However, since MMT has a propensity to swell in water, it may undergo swelling when combined with natural polysaccharides. Additionally, it can potentially form hydrogen bonds with natural polysaccharides, leading to structural alterations.[36,37,39,40,42] The relationship between the G' and G'' moduli values, which show different trends depending on the

Table 1. G', G'', and G'/G'' Values and the Strain % Reversed Point of Doxorubicin-Loaded Polysaccharide Hydrogels (n = 1)

polysaccharides	G'	G''	G'/G''	strain (%) (G'/G'' < 1)
cellulose	2176.7	431.32	5.05	1.03
cellulose-MMT	2047.9	401.64	5.10	0.64
chitin	154.67	19.487	7.37	0.41
chitin-MMT	114.40	17.929	6.38	0.41
chitosan	247.38	19.392	12.76	1.61
chitosan-MMT	258.82	19.04	13.59	1.61
cellulose nanocrystal	217.38	16.77	15.40	1.00
cellulose nanocrystal-MMT	322.30	23.579	13.67	1.00

https://doi.org/10.1021/acsomega.3c08834
ACS Omega 2024, 9, 1936−1944

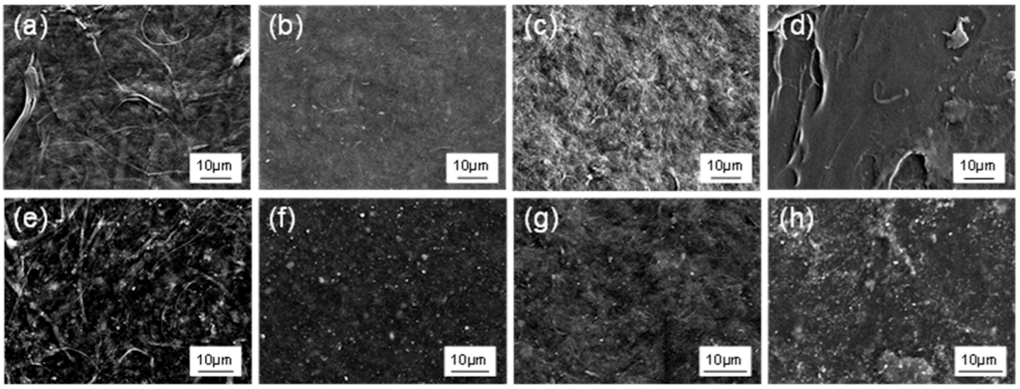

Figure 3. Scanning electron microscopy (SEM) images of doxorubicin-loaded natural composite films: (a) cellulose, (b) chitin, (c) chitosan, (d) cellulose nanocrystal, (e) cellulose-MMT, (f) chitin-MMT, (g) chitosan-MMT, and (h) cellulose nanocrystal-MMT.

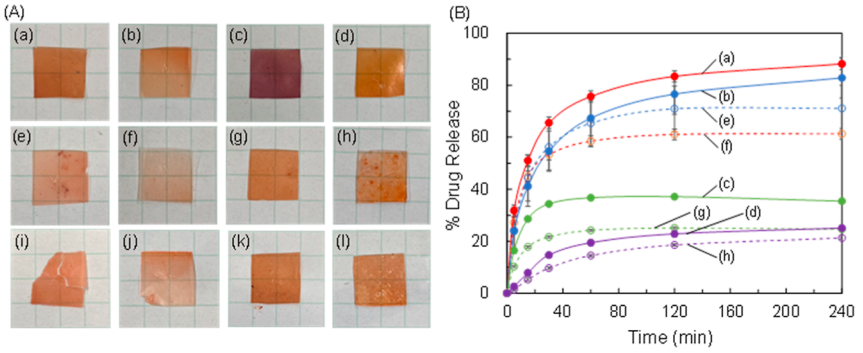

Figure 4. (A) Photograph of the doxorubicin-loaded natural composite films: (a) cellulose, (b) chitin, (c) chitosan, and (d) cellulose nanocrystal; photograph of the doxorubicin-loaded natural composite films after immersion in PBS for 240 min: (e) cellulose, (f) chitin, (g) chitosan, and (h) cellulose nanocrystal; photograph of the doxorubicin-loaded natural composite films with MMT after immersion in PBS for 240 min: (i) cellulose-MMT, (j) chitin-MMT, (k) chitosan-MMT, and (l) cellulose nanocrystal-MMT. (B) Drug-release ratio of doxorubicin-loaded natural composite films for 240 min ($n = 2$): (a) cellulose, (b) chitin, (c) chitosan, (d) cellulose nanocrystal, (e) cellulose-MMT, (f) chitin-MMT, (g) chitosan-MMT, and (h) cellulose nanocrystal-MMT.

type of polysaccharide, and the drug-release ratio/rate will be explained in more detail later.

Surface Observation of the Doxorubicin-Loaded Natural Composite Film. The morphologies of the doxorubicin-loaded polysaccharide film surface were observed (Figure 3a–d). Even though the doxorubicin-loaded polysaccharide films were prepared under the same drug amount as the nanofibers containing 2 wt %, the film surface morphology showed a difference. This can be attributed to the fact that each nanofiber has a different diameter or length, has different functional groups, and interacts with drugs. The doxorubicin-loaded cellulose film showed a remarkably large distribution of fiber lengths and diameters. In contrast, doxorubicin-loaded polysaccharide films with chitin and chitosan were uniform and thinner, and longer than those of cellulose, and the nanofiber diameter of the doxorubicin-loaded chitosan film was larger than that of the doxorubicin-loaded chitin film. The doxorubicin-loaded cellulose nanocrystal film showed an almost smooth surface. In the case of the surface of doxorubicin-loaded polysaccharide films with MMT, the diameter and length of the nanofibers showed no significant change with or without MMT. However, small dots, presumably consisting of MMT, including doxorubicin, can be observed (Figure 3e–h).

Drug–Release Behavior of the Doxorubicin-Loaded Natural Composite Film. The drug-release behavior was observed in natural polysaccharide films containing doxorubicin composed of cellulose, chitin, chitosan, and cellulose nanocrystals [Figure 4A(a–d)]. There seemed to be no significant change in the physical properties of the doxorubicin-loaded polysaccharide hydrogels depending on the presence or absence of MMT, but in the case of the doxorubicin-loaded chitosan film, a color change was observed in the form of the film after removing the solvent [Figure 4A(c,g,f)]. This is because the amine group of chitosan affects the charge transfer of doxorubicin and causes a color change from red to purple.[48] For the drug-release experiment on the doxorubicin-loaded polysaccharide films, when the films were immersed in phosphate-buffered saline (PBS), the color immediately changed from purple to red [Figure 4A(g)]. This is because the added PBS restores the transferred charge of doxorubicin to its original state. The doxorubicin release ratios from each film after immersion for 240 min were 88, 82, 35, and 25% in the order of cellulose, chitin, chitosan, and cellulose nanocrystal, respectively. This variation arises due to the distinct interaction forces that doxorubicin exhibits, such as hydrogen bonding and electrostatic interactions, with different natural polysaccharides. Furthermore, even though the quantitative composition of the films remains consistent, the dissimilarity in the length or diameter of the nanofibers comprising each film could also contribute to the variance in drug release quantities.

For a more detailed analysis, fitting was performed to confirm the drug-release rate for each release time interval, and

https://doi.org/10.1021/acsomega.3c08834
ACS Omega 2024, 9, 1936–1944

the slope (drug-release ratio/time = release rate) was obtained (Figure 5). The doxorubicin-loaded cellulose film with the highest release amount was released at the fastest rate, and the doxorubicin-loaded cellulose nanocrystal film was released at almost 1/10 rate compared to other polysaccharide films. The drug-release rate of the doxorubicin-loaded polysaccharide film with cellulose, chitin, and chitosan decreased over time; in particular, the chitosan film showed a rapid release rate change. The doxorubicin-loaded chitosan film was released rapidly for up to 5 min. The release amount rapidly decreased after 15 min, and almost no drug-release behavior was shown after 30 min. Meanwhile, in the case of the doxorubicin-loaded cellulose nanocrystal film, the release rate increased up to 15 min and significantly decreased after 1 h. The drug-release ratio and the change in the drug-release rate for each section differed depending on the type of the doxorubicin-loaded polysaccharide film. When MMT was added, the amount of drug released after 4 h was reduced from 88 to 61%, from 82 to 71%, from 35 to 25%, and from 25 to 21% in cellulose, chitin, chitosan, and cellulose nanocrystal, respectively. The reduction in the overall drug release attributed to the inclusion of MMT can be attributed to the subsequent interaction between MMT and doxorubicin. The drug-release rates were determined by analyzing the ratio of doxorubicin release from polysaccharide films at different time points: 0, 5, 15, 30, and 60 min. Although the release ratios of doxorubicin-loaded polysaccharide films decreased overall with the addition of MMT, the gap in the drug-release ratio was the highest in the doxorubicin-loaded cellulose film. When the drug-release rates across different sections were compared, it was observed that adding MMT generally decreased the release rate. However, the final release ratio decreased in the doxorubicin-loaded chitin film, like for other polysaccharide films. Interestingly, the drug-release rate for the doxorubicin-loaded chitin film was high for the initial 15 min, contrary to the behavior observed in other polysaccharide films. The rheological analysis revealed a change in the strain reversal point from 1.03 to 0.64%; in the case of the doxorubicin-loaded chitosan film, which had the highest strain reversal point of 1.61%, most of the drugs were released at 5 min, and the release rate rapidly slowed down after that. In the case of the doxorubicin-loaded chitin film, the strain reversal point is the smallest at 0.4%, and the release rate is the highest ever at 30 min regardless of the presence or absence of MMT, which means that the release continued (Table S2).

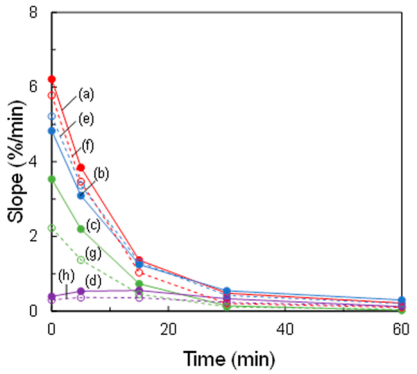

Figure 5. Drug release rate of the doxorubicin-loaded polysaccharides film (n = 2): (a) cellulose, (b) chitin, (c) chitosan, (d) cellulose nanocrystal, (e) cellulose-MMT, (f) chitin-MMT, (g) chitosan-MMT, and (h) cellulose nanocrystal-MMT.

Analyzing the Drug−Release Mechanism Using Korsmeyer−Peppas Models. The drug-release results were analyzed using the Higuchi, zero-order, first-order, and Korsmeyer−Peppas models, as listed in Tables 2 and S3.[34,46,47] The presumption of a zero-order model remains accurate solely for an extremely gradual drug release. However, in the context of the doxorubicin-loaded polysaccharide films, the release of doxorubicin occurred swiftly. It did not fit well. The application of a first-order model is appropriate for water-soluble drugs; however, the model drug doxorubicin exhibits hydrophobic characteristics. The Higuchi model is a modeling approach employed to elucidate the temporal dynamics of drug release. It is particularly applicable in scenarios in which the drug undergoes diffusion within a solid or gel matrix. Nevertheless, unlike the conventional situation where drugs disperse gradually within solid or gel-based dosage forms, the doxorubicin-loaded polysaccharide films exhibited a propensity to release a notable quantity rapidly in the initial stages. Consequently, the fitting outcomes were not congruent. The Korsmeyer−Peppas models provided a better description for doxorubicin release, except for the doxorubicin-loaded cellulose nanocrystal films with/without MMT. The n value was significantly below 0.5, suggesting that the drug underwent partial diffusion through the swollen film or that water filled the pores.[34] In the case of the doxorubicin-loaded chitosan films, the rapid initial diffusion is likely associated with a small R^2 value. Initially, the rapid and substantial diffusion of the drug led to a decline in its release as time progressed.

Table 2. Drug-Release Korsmeyer−Peppas Model Parameters

polysaccharides	Korsmeyer−Peppas		
	K	n	R^2
cellulose	23.38	0.262	0.921
cellulose-MMT	23.49	0.201	0.818
chitin	16.28	0.322	0.941
chitin-MMT	19.05	0.273	0.861
chitosan	15.19	0.188	0.712
chitosan-MMT	15.19	0.218	0.799
cellulose nanocrystal	1.44	0.581	0.889
cellulose nanocrystal-MMT	0.67	0.695	0.914

Skin Permeation Test of Doxorubicin-Loaded Cellulose Films. To confirm the amount of drug skin permeation, a skin permeation test of doxorubicin-loaded cellulose films with the highest release ratio was carried out. Figure 6A shows a photograph of the skin permeation experiment. The fluorescence intensity of doxorubicin was analyzed from a peak at 550 nm. From the slope of the approximation line in Figure 6B, we calculated the skin permeation rate, which was about 0.0345 μg/(cm^2·h). The doxorubicin permeation ratio was 0.598% (18 h), 0.620% (24 h), and 1.173% (48 h), respectively. The theoretical permeation rate was about 290 μg/(cm^2·h). With the doxorubicin-loaded cellulose films, it is estimated that it may take about 50 days for all the released doxorubicin to permeate (Figure S4).

CONCLUSIONS

We studied the control of the drug-release behavior using doxorubicin-loaded natural composite hydrogels. By incorpo-

https://doi.org/10.1021/acsomega.3c08834
ACS Omega 2024, 9, 1936−1944

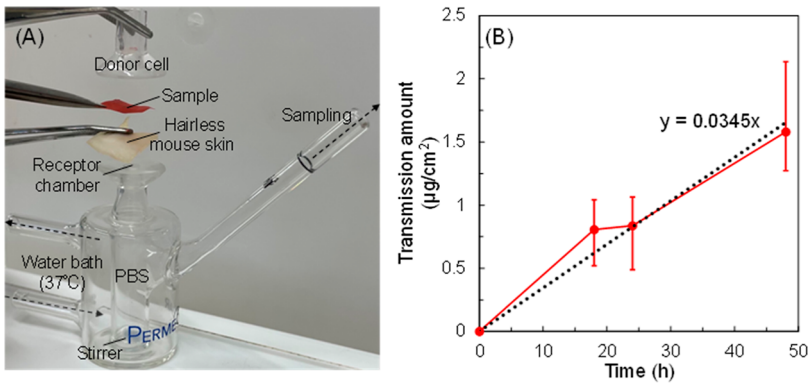

Figure 6. (A) Photograph of the skin permeation experiment. (B) Skin penetration amount of doxorubicin released from the doxorubicin-loaded cellulose film at 18, 24, and 48 h. (n = 3) (red: experimental data, black dot: theoretical data).

rating different types of natural polysaccharides and complex gels with natural minerals, we aimed to regulate the drug-release rate and the release ratio. Additionally, we examined the relationship between the mechanical properties of the doxorubicin-loaded natural composite hydrogels and their drug-release behaviors. Despite using the same amount of doxorubicin-containing composite hydrogels, the drug-release ratios ranged from 21 to 88%. This is because each nanofiber has a different diameter or length, has different functional groups, and interacts with doxorubicin. Moreover, the incorporation of natural minerals resulted in a reduction in the drug-release ratio from 27% to below 10%. This is because MMTs adsorbed doxorubicin, making it difficult to release it. Although the amount of drug release appears to decrease when observed in the short term, this means that continuous release is possible from a long-term perspective. This is the reason for adding MMT. The presence of MMT leads to a decrease of approximately 10% in the drug release ratio, which is equivalent to 16 μg of DOX. Therefore, the time required for this amount of DOX to permeate the skin is approximately 19 days. Furthermore, we observed that the drug-release rate varied across different sections depending on the type of natural polysaccharide used. The Korsmeyer−Peppas model was fitted to account for the nonlinear drug release of solid or gel drug formulations. This means that they can be usefully used in applications related to oral or transdermal drug administration. In the final stage of our study, we evaluated the potential of doxorubicin-loaded cellulose film as a drug seal by testing its skin permeation properties.

■ ASSOCIATED CONTENT

Supporting Information

The Supporting Information is available free of charge at https://pubs.acs.org/doi/10.1021/acsomega.3c08834.

Standard curve of free DOX, photograph of the doxorubicin-loaded polysaccharide hydrogels with MMT, and rheological properties of the doxorubicin-loaded polysaccharide hydrogels with MMT (PDF)

■ AUTHOR INFORMATION

Corresponding Author

Ji Ha Lee − *Chemical Engineering Program, Graduate School of Advanced Science and Engineering, Hiroshima University, Higashi-Hiroshima 739-8527, Japan*; orcid.org/0000-0002-4456-0128; Email: leejiha@hiroshima-u.ac.jp

Authors

Hiroya Tsubota − *Chemical Engineering Program, Graduate School of Advanced Science and Engineering, Hiroshima University, Higashi-Hiroshima 739-8527, Japan*

Tomoyuki Tachibana − *Chemical Engineering Program, Graduate School of Advanced Science and Engineering, Hiroshima University, Higashi-Hiroshima 739-8527, Japan*

Complete contact information is available at: https://pubs.acs.org/10.1021/acsomega.3c08834

Author Contributions

The manuscript was written through contributions of all authors. All authors have given approval to the final version of the manuscript.

Notes

The authors declare no competing financial interest.

■ ACKNOWLEDGMENTS

This work was supported by MEXT Promotion of Distinctive Joint Research Center Program (grant no. JPMXP 0621467946).

■ REFERENCES

(1) Zhang, Y.; Dong, L.; Liu, L.; Wu, Z.; Pan, D.; Liu, L. Recent Advances of Stimuli-Responsive Polysaccharide Hydrogels in Delivery Systems: A Review. *J. Agric. Food Chem.* **2022**, *70*, 6300−6316.

(2) Hu, J. L.; Nie, S. P.; Wu, Q. M.; Li, C.; Fu, Z. H.; Gong, J.; Cui, S. W.; Xie, M. Y. Polysaccharide from Seeds of Plantago aAsiatica L. Affects Lipid Metabolism and Colon Microbiota of Mouse. *J. Agric. Food Chem.* **2014**, *62* (1), 229−234.

(3) Rutenberg, R.; Galaktionova, D.; Golden, G.; Cohen, Y.; Levi-Kalisman, Y.; Cohen, G.; Král, P.; Poverenov, E. Omniphilic Polysaccharide-Based Nanocarriers for Modular Molecular Delivery in a Broad Range of Biosystems. *ACS Appl. Mater. Interfaces* **2018**, *10* (43), 36711−36720.

(4) Zhang, M.; Ma, Y.; Wang, Z.; Han, Z.; Gao, W.; Zhou, Q.; Gu, Y. A CD44-Targeting Programmable Drug Delivery System for Enhancing and Sensitizing Chemotherapy to Drug-Resistant Cancer. *ACS Appl. Mater. Interfaces* **2019**, *11*, 5851−5861.

(5) Akasov, R.; Borodina, T.; Zaytseva, E.; Sumina, A.; Bukreeva, T.; Burov, S.; Markvicheva, E. Ultrasonically Assisted Polysaccharide Microcontainers for Delivery of Lipophilic Antitumor Drugs: Preparation and in Vitro Evaluation. *ACS Appl. Mater. Interfaces* **2015**, *7* (30), 16581−16589.

(6) Lai, W. F.; Shum, H. C. Hypromellose-Graft-Chitosan and Its Polyelectrolyte Complex as Novel Systems for Sustained Drug Delivery. *ACS Appl. Mater. Interfaces* **2015**, *7* (19), 10501−10510.

(7) Stana, J.; Stergar, J.; Gradišnik, L.; Flis, V.; Kargl, R.; Fröhlich, E.; Stana Kleinschek, K.; Mohan, T.; Maver, U. Multilayered Polysaccharide Nanofilms for Controlled Delivery of Pentoxifylline and Possible Treatment of Chronic Venous Ulceration. *Biomacromolecules* **2017**, *18* (9), 2732−2746.
(8) Kamra, M.; Moitra, P.; Ponnalagu, D.; Karande, A. A.; Bhattacharya, S. New Water-Soluble Oxyamino Chitosans as Biocompatible Vectors for Efficacious Anticancer Therapy via Co-Delivery of Gene and Drug. *ACS Appl. Mater. Interfaces* **2019**, *11* (41), 37442−37460.
(9) Ma, Y.; Björnmalm, M.; Wise, A. K.; Cortez-Jugo, C.; Revalor, E.; Ju, Y.; Feeney, O. M.; Richardson, R. T.; Hanssen, E.; Shepherd, R. K.; Porter, C. J. H.; Caruso, F. Gel-Mediated Electrospray Assembly of Silica Supraparticles for Sustained Drug Delivery. *ACS Appl. Mater. Interfaces* **2018**, *10* (37), 31019−31031.
(10) Zhang, J.; Choi, Y. S.; Yoo, C. G.; Kim, T. H.; Brown, R. C.; Shanks, B. H. Cellulose-Hemicellulose and Cellulose-Lignin Interactions during Fast Pyrolysis. *ACS Sustain. Chem. Eng.* **2015**, *3* (2), 293−301.
(11) Tang, L.; Weder, C. Cellulose Whisker/Epoxy Resin Nanocomposites. *ACS Appl. Mater. Interfaces* **2010**, *2* (4), 1073−1080.
(12) Del Valle, L. J.; Díaz, A.; Puiggalí, J. Hydrogels for Biomedical Applications: Cellulose, Chitosan, and Protein/Peptide Derivatives. *Gels* **2017**, *3*, 27.
(13) Marangon, C. A.; Martins, V. C. A.; Ling, M. H.; Melo, C. C.; Plepis, A. M. G.; Meyer, R. L.; Nitschke, M. Combination of Rhamnolipid and Chitosan in Nanoparticles Boosts Their Antimicrobial Efficacy. *ACS Appl. Mater. Interfaces* **2020**, *12* (5), 5488−5499.
(14) Yang, X.; Tu, Y.; Li, L.; Shang, S.; Tao, X. M. Well-Dispersed Chitosan/Graphene Oxide Nanocomposites. *ACS Appl. Mater. Interfaces* **2010**, *2* (6), 1707−1713.
(15) Ayoub, A.; Venditti, R. A.; Pawlak, J. J.; Salam, A.; Hubbe, M. A. Novel Hemicellulose-Chitosan Biosorbent for Water Desalination and Heavy Metal Removal. *ACS Sustain. Chem. Eng.* **2013**, *1* (9), 1102−1109.
(16) Lee, J. H.; Tachibana, T.; Wadamori, H.; Yamana, K.; Kawasaki, R.; Kawamura, S.; Isozaki, H.; Sakuragi, M.; Akiba, I.; Yabuki, A. Drug-Loaded Biocompatible Chitosan Polymeric Films with Both Stretchability and Controlled Release for Drug Delivery. *ACS Omega* **2022**, *8*, 1282−1290.
(17) King, C. A.; Shamshina, J. L.; Zavgorodnya, O.; Cutfield, T.; Block, L. E.; Rogers, R. D. Porous Chitin Microbeads for More Sustainable Cosmetics †. *ACS Sustain. Chem. Eng.* **2017**, *5* (12), 11660−11667.
(18) Pierson, Y.; Chen, X.; Bobbink, F. D.; Zhang, J.; Yan, N. Acid-Catalyzed Chitin Liquefaction in Ethylene Glycol. *ACS Sustain. Chem. Eng.* **2014**, *2* (8), 2081−2089.
(19) Duan, Y.; Freyburger, A.; Kunz, W.; Zollfrank, C. Lignin/Chitin Films and Their Adsorption Characteristics for Heavy Metal Ions. *ACS Sustain. Chem. Eng.* **2018**, *6* (5), 6965−6973.
(20) Zhu, C.; Liu, P.; Mathew, A. P. Self-Assembled TEMPO Cellulose Nanofibers: Graphene Oxide-Based Biohybrids for Water Purification. *ACS Appl. Mater. Interfaces* **2017**, *9* (24), 21048−21058.
(21) Zhu, L.; Zong, L.; Wu, X.; Li, M.; Wang, H.; You, J.; Li, C. Shapeable Fibrous Aerogels of Metal-Organic-Frameworks Templated with Nanocellulose for Rapid and Large-Capacity Adsorption. *ACS Nano* **2018**, *12* (5), 4462−4468.
(22) Filpponen, I.; Argyropoulos, D. S. Regular Linking of Cellulose Nanocrystals via Click Chemistry: Synthesis and Formation of Cellulose Nanoplatelet Gels. *Biomacromolecules* **2010**, *11* (4), 1060−1066.
(23) Rahmatika, A. M.; Goi, Y.; Kitamura, T.; Widiyastuti, W.; Ogi, T. TEMPO-Oxidized Cellulose Nanofiber (TOCN) Decorated Macroporous Silica Particles: Synthesis, Characterization, and Their Application in Protein Adsorption. *Mater. Sci. Eng. C* **2019**, *105*, 110033.
(24) Lee, J. H.; Gustin, J. P.; Chen, T.; Payne, G. F.; Raghavan, S. R. Vesicle-Biopolymer Gels: Networks of Surfactant Vesicles Connected by Associating Biopolymers. *Langmuir* **2005**, *21* (1), 26−33.
(25) Li, M. C.; Wu, Q.; Song, K.; Lee, S.; Qing, Y.; Wu, Y. Cellulose Nanoparticles: Structure-Morphology-Rheology Relationships. *ACS Sustain. Chem. Eng.* **2015**, *3* (5), 821−832.
(26) Cao, R.; Kumar, D.; Dinsmore, A. D. Vesicle-Based Gel via Polyelectrolyte-Induced Adhesion: Structure, Rheology, and Response. *Langmuir* **2021**, *37* (5), 1714−1724.
(27) Li, K.; Chen, X.; Wang, Y.; Sun, B.; Yuan, Z.; Liu, Y. Regenerated Cellulose Microgel: A Promising Reinforcing Agent and Gelator for Soft Matter. *ACS Appl. Polym. Mater.* **2021**, *3* (8), 4101−4108.
(28) Kowalczuk, J.; Bielejewski, M.; Łapiński, A.; Luboradzki, R.; Tritt-Goc, J. The Solvent-Gelator Interaction as the Origin of Different Diffusivity Behavior of Diols in Gels Formed with Sugar-Based Low-Molecular-Mass Gelator. *J. Phys. Chem. B* **2014**, *118* (14), 4005−4015.
(29) Sultana, R.; Di Domenico, F.; Tseng, M.; Cai, J.; Noel, T.; Chelvarajan, R. L.; Pierce, W. D.; Cini, C.; Bondada, S.; St. Clair, D. K.; Butterfield, D. A. Doxorubicin-Induced Thymus Senescence. *J. Proteome Res.* **2010**, *9* (12), 6232−6241.
(30) Cha, G. D.; Lee, W. H.; Sunwoo, S. H.; Kang, D.; Kang, T.; Cho, K. W.; Kim, M.; Park, O. K.; Jung, D.; Lee, J.; Choi, S. H.; Hyeon, T.; Kim, D. H. Multifunctional Injectable Hydrogel for in Vivo Diagnostic and Therapeutic Applications. *ACS Nano* **2022**, *16* (1), 554−567.
(31) Wu, W.; Chen, H.; Shan, F.; Zhou, J.; Sun, X.; Zhang, L.; Gong, T. A Novel Doxorubicin-Loaded in Situ Forming Gel Based High Concentration of Phospholipid for Intratumoral Drug Delivery. *Mol. Pharm.* **2014**, *11* (10), 3378−3385.
(32) Peng, C. L.; Shih, Y. H.; Liang, K. S.; Chiang, P. F.; Yeh, C. H.; Tang, I. C.; Yao, C. J.; Lee, S. Y.; Luo, T. Y.; Shieh, M. J. Development of in Situ Forming Thermosensitive Hydrogel for Radiotherapy Combined with Chemotherapy in a Mouse Model of Hepatocellular Carcinoma. *Mol. Pharm.* **2013**, *10* (5), 1854−1864.
(33) Biswas, A.; Ghosh, T.; Gavel, P. K.; Das, A. K. PEG Functionalized Stimuli Responsive Self-Healable Injectable Dynamic Imino-Boronate G-Quadruplex Hydrogel for the Delivery of Doxorubicin. *ACS Appl. Bio Mater.* **2020**, *3* (2), 1052−1060.
(34) Lee, J. H.; Tachibana, T.; Yamana, K.; Kawasaki, R.; Yabuki, A. Simple Formation of Cancer Drug-Containing Self-Assembled Hydrogels with Temperature and PH-Responsive Release. *Langmuir* **2021**, *37* (38), 11269−11275.
(35) Jantarat, C.; Muenraya, P.; Srivaro, S.; Nawakitrangsan, A.; Promsornpason, K. Comparison of Drug Release Behavior of Bacterial Cellulose Loaded with Ibuprofen and Propranolol Hydrochloride. *RSC Adv.* **2021**, *11* (59), 37354−37365.
(36) Li, Y.; Chen, M.; Song, H.; Yuan, P.; Zhang, B.; Liu, D.; Zhou, H.; Bu, H. Effect of Cations (Na+, K+, and Ca2+) on Methane Hydrate Formation on the External Surface of Montmorillonite: Insights from Molecular Dynamics Simulation. *ACS Earth Space Chem.* **2020**, *4* (4), 572−582.
(37) Liu, M. L.; Huang, M.; Tian, L. Y.; Zhao, L. H.; Ding, B.; Kong, D. B.; Yang, Q. H.; Shao, J. J. Two-Dimensional Nanochannel Arrays Based on Flexible Montmorillonite Membranes. *ACS Appl. Mater. Interfaces* **2018**, *10* (51), 44915−44923.
(38) Martín-Alfonso, M. A.; Rubio-Valle, J. F.; Hinestroza, J. P.; Martín-Alfonso, J. E. Impact of Vegetable Oil Type on the Rheological and Tribological Behavior of Montmorillonite-Based Oleogels. *Gels* **2022**, *8* (8), 504.
(39) Sun, L.; Hirvi, J. T.; Schatz, T.; Kasa, S.; Pakkanen, T. A. Estimation of Montmorillonite Swelling Pressure: A Molecular Dynamics Approach. *J. Phys. Chem. C* **2015**, *119* (34), 19863−19868.
(40) Sreekanth Reddy, O.; Subha, M. C. S.; Jithendra, T.; Madhavi, C.; Chowdoji Rao, K. Curcumin Encapsulated Dual Cross Linked Sodium Alginate/Montmorillonite Polymeric Composite Beads for Controlled Drug Delivery. *J. Pharm. Anal.* **2021**, *11* (2), 191−199.
(41) Wang, R.; Peng, Y.; Zhou, M.; Shou, D. Smart Montmorillonite-Polypyrrole Scaffolds for Electro-Responsive Drug Release. *Appl. Clay Sci.* **2016**, *134*, 50−54.

https://doi.org/10.1021/acsomega.3c08834
ACS Omega 2024, 9, 1936−1944

(42) Hellrup, J.; Holmboe, M.; Nartowski, K. P.; Khimyak, Y. Z.; Mahlin, D. Structure and Mobility of Lactose in Lactose/Sodium Montmorillonite Nanocomposites. *Langmuir* **2016**, *32* (49), 13214−13225.
(43) Kochkina, N. E.; Butikova, O. A.; Lukin, N. D. A Study of Films Based on Starch and Na-Montmorillonite Designed for Prolonged Release of Oxytetracycline Hydrochloride. *Starch/Staerke* **2021**, *73* (7−8), 2100014.
(44) Altunkaynak, F.; Okur, M.; Saracoglu, N. Controlled Release of Paroxetine from Chitosan/Montmorillonite Composite Films. *J. Drug Deliv. Sci. Technol.* **2022**, *68*, 103099.
(45) Wong, H. M.; Wang, J. J.; Wang, C. H. In Vitro Sustained Release of Human Immunoglobulin G from Biodegradable Microspheres. *Ind. Eng. Chem. Res.* **2001**, *40* (3), 933−948.
(46) Monton, C.; Sampaopan, Y.; Pichayakorn, W.; Panrat, K.; Suksaeree, J. Herbal Transdermal Patches Made from Optimized Polyvinyl Alcohol Blended Film: Herbal Extraction Process, Film Properties, and in Vitro Study. *J. Drug Deliv. Sci. Technol.* **2022**, *69*, 103170.
(47) Aycan, D.; Yayla, N. A.; Aydin, Y. A. Chitosan Polyvinyl Alcohol Blend Films for Ibuprofen Encapsulation: Fabrication, Characterization and Kinetics. *Polym. Degrad. Stab.* **2020**, *181*, 109346.
(48) Jeong, C.; Kim, J.; Kim, Y. C. Fluorescence Color-Changeable Branched-Form Heptamethine Cyanine Dye as a Redox-Responsive Multi-Functional Drug Delivery System for Enhanced Cancer Diagnosis and Chemophototherapy. *J. Ind. Eng. Chem.* **2020**, *87*, 187−197.

https://doi.org/10.1021/acsomega.3c08834
ACS Omega 2024, 9, 1936−1944